Hydrodynamic optical soliton tunneling

P. Sprenger,[1,*] M. A. Hoefer,[1,†] and G. A. El[2,‡]

[1]*Department of Applied Mathematics, University of Colorado, Boulder, Colorado 80309, USA*
[2]*Department of Mathematical Sciences, Loughborough University, Loughborough LE11 3TU, United Kingdom*

A notion of hydrodynamic optical soliton tunneling is introduced in which a dark soliton is incident upon an evolving, broad potential barrier that arises from an appropriate variation of the input signal. The barriers considered include smooth rarefaction waves and highly oscillatory dispersive shock waves. Both the soliton and the barrier satisfy the same one-dimensional defocusing nonlinear Schrödinger (NLS) equation, which admits a convenient dispersive hydrodynamic interpretation. Under the scale separation assumption of nonlinear wave (Whitham) modulation theory, the highly nontrivial nonlinear interaction between the soliton and the evolving hydrodynamic barrier is described in terms of self-similar, simple wave solutions to an asymptotic reduction of the Whitham-NLS partial differential equations. One of the Riemann invariants of the reduced modulation system determines the characteristics of a soliton interacting with a mean flow that results in soliton tunneling or trapping. Another Riemann invariant yields the tunneled soliton's phase shift due to hydrodynamic interaction. Soliton interaction with hydrodynamic barriers gives rise to effects that include reversal of the soliton propagation direction and spontaneous soliton cavitation, which further suggest possible methods of dark soliton control in optical fibers.

I. INTRODUCTION

The tunneling of wave packets incident upon a potential barrier is a defining quantum mechanical property [1]. The linear phenomenon can be extended to nonlinear solitonic wave packets or solitons—localized, unchanging waveforms in which nonlinear and dispersive effects are in balance. In the original consideration of a soliton incident upon a potential barrier, it was found that the soliton can losslessly pass, or tunnel, through a localized repulsive or attractive potential [2]. The connection of this so-called soliton tunneling with quantum mechanical tunneling was established in an optical setting in Ref. [3] where a bright optical pulse propagating in an optical fiber with anomolous dispersion was transmitted through a localized defective region of normal dispersion—the analog of a potential barrier.

Soliton tunneling has been studied theoretically recently in various physical systems including optical media [4–7], nematic liquid crystals [8,9], and matter waves in Bose-Einstein condensates (BECs) [10,11]. Recent experiments observed the nonlinear analogs of some linear quantum features including nonlinear scattering [12], reflection and ejection [13], and soliton tunneling [14]. In a related vein, analogies between soliton tunneling and other physical effects were considered in Refs. [15–17].

In the focusing (anomalous dispersion) regime, nonlinear optical plane wave propagation is subject to modulational instability with respect to long wavelength perturbations [18].

In contrast, plane wave propagation in the defocusing (normal dispersion) regime is stable and, remarkably, exhibits many features characteristic of fluid motion [19]. The dispersive effects in such a "fluid of light" are due to diffractive or chromatic properties of the medium. The dispersive hydrodynamic behavior of light propagation has been considered and observed in a number of works; see, e.g., Refs. [20–22].

Robust features of the diffraction of laser light in a nonlinear, defocusing medium and matter waves in a repulsive BEC include dark solitons, moving depression waves whose width is proportional to the coherence length l of the medium. In addition to solitons, these media also support spatially extended, smooth configurations that can exhibit wave breaking and the spontaneous emergence of highly oscillatory dispersive shock waves (DSWs) [23]. Optical DSWs have been observed in both bulk media [20] and optical fibers [24]. While the DSW oscillatory length scale is also the medium's microscopic coherence length l, DSWs exhibit expanding, rank-ordered oscillations spanning a larger, macroscopic coherence length scale L, which increases with time. This latter length scale also characterizes nonoscillatory hydrodynamic flows such as expansion or rarefaction waves (RWs) and compressive Riemann waves that have recently been observed in optical fibers in the context of wave-breaking control [25]. The scale separation $l \ll L$, a natural characterization of dispersive hydrodynamics [26], enables a mathematical description of DSWs via nonlinear wave, Whitham averaging [23,27], while RWs are described by the long-wave (hydrodynamic), dispersionless limit of the original equations.

Despite the fact that solitons, RWs, and DSWs are well known, fundamental features of dispersive media, soliton-RW, and soliton-DSW interactions have been mostly overlooked. As we show, these interactions motivate an alternative notion

---
*patrick.sprenger@colorado.edu
†hoefer@colorado.edu
‡g.el@lboro.ac.uk

of optical tunneling whereby a dark soliton incident upon a spatially extended hydrodynamic barrier in the form of a DSW or a RW can penetrate through to the other side of the evolving hydrodynamic structure. Thus, in contrast to the traditional notion of soliton tunneling through an externally imposed barrier, hydrodynamic soliton tunneling corresponds to the full penetration and emergence of the soliton through an intrinsic hydrodynamic state that evolves *according to the same equation as the soliton*. This generalizes the understanding of a soliton as a coherent, particle-like entity that can interact elastically with other solitons [28] and dispersive radiation [29] to one that can also interact with nonlinear hydrodynamic states and emerge intact, i.e., without fissioning or radiation, albeit with a different amplitude that results from a change in the background mean flow.

In this paper, we analyze the tunneling of solitons through hydrodynamic states within the framework of the integrable, defocusing nonlinear Schrödinger (NLS) equation, which is an accurate model for nonlinear light propagation in single mode optical fibers with normal dispersion [30]. We invoke the scale separation $l \ll L$ inherent to Whitham modulation theory in order to derive a system of asymptotic equations that describe the interaction between narrow dark solitons and evolving, broad hydrodynamic barriers. We obtain the conditions on the incident soliton amplitude and hydrodynamic mean flow density and velocity for tunneling. One of the fundamental properties of hydrodynamic soliton tunneling is *hydrodynamic reciprocity* whereby the tunneling through RWs and DSWs is described by the same set of conditions in spite of the very different interaction dynamics. This general property of *solitonic hydrodynamics* has been recently formulated and experimentally confirmed for a fluid system [31]. We also show that tunneling is not always possible and that the soliton can be absorbed or trapped within the hydrodynamic flow. Moreover, we find that soliton interaction with hydrodynamic states can lead to reversal of the soliton's propagation direction and spontaneous soliton cavitation.

Our analysis can be applied to a large class of dispersive hydrodynamic systems, including dispersive Eulerian equations [23,32] which have broad applications. The particular case of optical hydrodynamic soliton tunneling considered here could be observed, for example, within the experimental setting described in Ref. [22] for the generation of DSWs and RWs in optical fibers. This work generalizes unidirectional solitonic hydrodynamics to the optical setting where waves can propagate bidirectionally.

II. PROBLEM FORMULATION

We consider the defocusing NLS equation

$$i\psi_t = -\frac{1}{2}\psi_{xx} + |\psi|^2\psi, \qquad (1)$$

where in the context of fiber optic propagation, t is the longitudinal coordinate in the fiber, x is the retarded time, and $\psi(x,t)$ is the complex-valued, slowly varying envelope of the electric field. All variables are nondimensionalized to their typical values. See, e.g., Ref. [22] for a detailed description of NLS normalizations and typical values of physical parameters pertinent to the regimes considered here.

Equation (1) can be written in dispersive hydrodynamic form via the transformation $\psi = \sqrt{\rho}e^{i\phi}$, $u = \phi_x$:

$$\rho_t + (\rho u)_x = 0, \quad u_t + uu_x + \rho_x = \left(\frac{\rho_{xx}}{4\rho} - \frac{\rho_x^2}{8\rho^2}\right)_x, \quad (2)$$

where ρ is the optical power and u is the chirp. In terms of the hydrodynamic interpretation of these quantities, we will refer to ρ as a mass density and u as a flow velocity (see, e.g., Ref. [23]). Within this setting, the normalized coherence length is $l = \rho_0^{-1/2}$ where ρ_0 is a typical density scale. The coherence length is an intrinsic scale that, along with the coherence time $\tau = \rho_0^{-1}$, corresponds to a scaling invariance of the hydrodynamic equations (2). In BECs, l is known as the healing length [33].

Equation (2) admits the localized, dark soliton solution

$$\rho(x,t) = \overline{\rho} - a\,\mathrm{sech}^2[\sqrt{a}(x - ct - x_0)],$$
$$u(x,t) = \overline{u} \pm \sqrt{\overline{\rho} - a}[1 - \overline{\rho}/\rho(x,t)],$$
$$c = \overline{u} \pm \sqrt{\overline{\rho} - a}, \qquad (3)$$

where a is the maximum deviation from the mean density $\overline{\rho}$, $\overline{u}$ is the mean flow velocity, and c is the soliton amplitude-speed relation. The $\pm$ in (3) is due to the bidirectional nature of the NLS equation as a dispersive hydrodynamic system (2). When $a = \overline{\rho}$, the soliton is called a black soliton because its minimum is a zero density, cavitation point.

The typical tunneling problem consists of a soliton incident on a fixed potential barrier, either due to a change in the medium or an external effect. However, the spatio-temporal barriers considered here evolve according to the same equation that describes the dynamics of the medium. For an optical fiber with homogeneous, normal dispersion, this corresponds to a time-dependent input signal that results in both a soliton and a large-scale barrier. We assume that the hydrodynamic mean flow $(\overline{\rho}, \overline{u})$ that develops from the initial data varies on much longer length and time scales $L \gg l$, $T \gg \tau$, respectively. In this regime, the third order dispersive term in (2) is negligible, resulting in the long-wave, dispersionless, quasilinear equations for the mean flow $\rho \to \overline{\rho}$, $u \to \overline{u}$:

$$\overline{r}_t + \frac{1}{2}(3\overline{r} + \overline{s})\overline{r}_x = 0, \quad \overline{s}_t + \frac{1}{2}(\overline{r} + 3\overline{s})\overline{s}_x = 0, \quad (4)$$

written in diagonal form where

$$\overline{r} = \overline{u}/2 - \sqrt{\overline{\rho}}, \quad \overline{s} = \overline{u}/2 + \sqrt{\overline{\rho}} \qquad (5)$$

are the Riemann invariants. In fact, Eqs. (4) are the shallow water equations in one dimension, and RWs are determined exclusively by the constancy of $\overline{r}$ or $\overline{s}$ [34]. Remarkably, the same constant Riemann invariant determines the loci of simple wave DSWs [23], in contrast to viscous shock waves of classical fluid dynamics, whose loci are determined by the Rankine-Hugoniot conditions [34].

We consider the problem of a dark soliton (3) incident upon a barrier that evolves from step initial data in the mean flow $\overline{\rho}(x,0)$, $\overline{u}(x,0)$, where

$$\overline{\rho}(x,0) = \begin{cases} \overline{\rho}_- & x < 0 \\ \overline{\rho}_+ & x > 0 \end{cases}, \quad \overline{u}(x,0) = \begin{cases} \overline{u}_- & x < 0 \\ \overline{u}_+ & x > 0 \end{cases}. \quad (6)$$
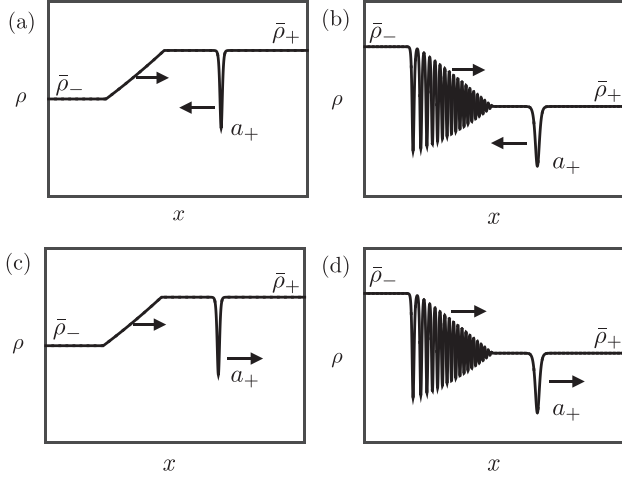
FIG. 1. Hydrodynamic soliton tunneling configurations: (a) soliton-RW collision, (b) soliton-DSW collision, (c) RW overtaking soliton, (d) DSW overtaking soliton.

As we will show, the long-time evolution of soliton-hydrodynamic barrier interaction is determined by the far-field flow conditions $\bar{\rho}_{\pm}$ and $\bar{u}_{\pm}$. Therefore, our theory generalizes to soliton tunneling through arbitrary hydrodynamic barriers with given far-field conditions.

The step initial conditions (6) generally evolve into a combination of two waves: RWs and/or DSWs each characterized by a simple-wave locus of the dispersionless limit system (4) [23,35]. Therefore, we shall be imposing a simple-wave constraint on the initial mean flow data (6), i.e., we assume that either $\bar{r}(x,0)$ or $\bar{s}(x,0)$ found from (5) is constant across $x = 0$ so that the mean flow will evolve into a single expanding hydrodynamic wave, either a RW or a DSW. Due to the bidirectional nature of the NLS equation, there are four distinct configurations, defined by the direction of the jump (up or down) of the Riemann invariant $\bar{r}$ or $\bar{s}$ across $x = 0$. We will focus on the two cases that result in a RW or a DSW when $\bar{r}(x,0)$ is constant. These two configurations along with an incident dark soliton moving to the left or right define four basic cases of hydrodynamic soliton tunneling considered here and shown in Fig. 1.

We pause briefly to note some common terminology in the nonlinear waves literature [23]. The RW and DSW depicted in Fig. 1 are referred to as a 2-RW and a 2-DSW, respectively, because their characteristic wave speeds degenerate to the *fastest* long wave speed $\bar{u}_0 + \sqrt{\bar{\rho}_0}$ when $\bar{\rho}_+, \bar{\rho}_- \to \bar{\rho}_0$, $\bar{u}_+, \bar{u}_- \to \bar{u}_0$. The other two cases where $\bar{s}(x,0)$ is constant correspond to a 1-RW or a 1-DSW because their speeds degenerate to the slowest long wave speed $\bar{u}_0 - \sqrt{\bar{\rho}_0}$. These 1-waves can be obtained from the 2-waves considered here with the reflection invariance $x \to -x$, $u \to -u$ of Eqs. (2).

To describe how the mean flow couples to the soliton amplitude during the interaction, we utilize Whitham modulation theory [27]. The general framework for Whitham modulation theory encompasses slow modulation on the space and time scales L and T of a periodic wave's parameters, which lead to a system of quasilinear partial differential equations (PDEs) for the parameter evolution. For the NLS equation, the modulation equations are a system of four equations that can be written in diagonal form [23,36–38]:

$$\frac{\partial r_i}{\partial t} + V_i(\mathbf{r})\frac{\partial r_i}{\partial x} = 0, \quad i = 1, \dots, 4. \tag{7}$$

The Riemann invariants $\mathbf{r}$ satisfy $r_4 \geqslant r_3 \geqslant r_2 \geqslant r_1$ and vary on the much larger spatiotemporal scales L and T than the scales l and τ of the soliton (3). The characteristic velocities are computed via

$$V_i(\mathbf{r}) = \left(1 - \frac{\lambda}{\partial_i \lambda}\partial_i\right)U, \tag{8}$$

where $\partial_i = \frac{\partial}{\partial r_i}$, and

$$\lambda = \frac{2K(m)}{\sqrt{(r_4 - r_2)(r_3 - r_1)}}, \quad U = \frac{1}{2}\sum_{j=1}^{4}r_j \tag{9}$$

are the wavelength and phase velocity of the underlying cnoidal wave, respectively. Here $K(m)$ is the complete elliptic integral of the first kind and $m = [(r_2 - r_1)(r_4 - r_3)]/[(r_4 - r_2)(r_3 - r_1)]$. The characteristic velocities exhibit the ordering $V_i \leqslant V_j$ if $1 \leqslant i \leqslant j \leqslant 4$. The wave amplitude is $a = (r_2 - r_1)(r_4 - r_3)$. By setting all but one Riemann invariant constant, we obtain an equation for a simple wave of modulation, which we call a j-wave, where j is the index of the nonconstant, varying Riemann invariant.

Equation (7) is consistent with the wave conservation law:

$$k_t + (kU)_x = 0, \quad k = 2\pi/\lambda. \tag{10}$$

Soliton-mean field interaction is described by the soliton limit of the NLS-Whitham equation (7), which is achieved when $r_2 = r_3$ (see, e.g., Ref. [23]). By analyzing the expression (8) for the characteristic velocities in the soliton limit $r_2 = r_3$, it is possible to establish that the limiting modulation system consists of shallow water equations (6) where $\bar{s} = r_4$, $\bar{r} = r_1$ and the equation for the merged Riemann invariant r_3 is [23]

$$r_{3,t} + \frac{1}{2}(\bar{r} + 2r_3 + \bar{s})r_{3,x} = 0, \tag{11}$$

with

$$r_3 = \bar{u}/2 \pm \sqrt{\bar{\rho} - a}, \tag{12}$$

where the two signs are due to bidirectionality [cf. the second and third formulas in Eq. (3)].

Thus, effectively, Eq. (11) is the equation for the soliton amplitude $a(x,t)$. Crucially for our consideration, the soliton amplitude here is a spatio-temporal *field*, satisfying a PDE, while in standard soliton perturbation theories [39], the soliton amplitude has only a temporal dependence that satisfies an ODE along the soliton trajectory. The trajectory and dynamics of a single soliton from the amplitude field can be interpreted as the introduction of a fictitious train of noninteracting solitons of the same amplitude and some small wave number $0 < k \ll 1$, which necessarily satisfies the wave conservation equation (10) with $U = \frac{1}{2}(\bar{r} + 2r_3 + \bar{s}) = c$, the soliton amplitude-speed relation. Using the limiting system (4), (11), the wave conservation equation (10) can be written in diagonal, Riemann

invariant form:

$$(kp)_t + c(kp)_x = 0,$$

$$p = \exp\left[-\int_{\bar{s}_0}^{\bar{s}} \frac{\frac{dc_s}{d\bar{s}}}{\frac{1}{2}(\bar{r} + 3s) - c}\, ds\right], \qquad (13)$$

where $\bar{s}_0$ is some fixed reference value, e.g., $\bar{s}_-$.

Thus, the initial conditions (6) for the hydrodynamic barrier should be complemented by similar conditions for the soliton amplitude field and the small wave number,

$$a(x,0) = \begin{cases} a_- & x < 0 \\ a_+ & x > 0 \end{cases}, \quad k(x,0) = \begin{cases} k_- & x < 0 \\ k_+ & x > 0 \end{cases}, \quad (14)$$

where only the incident amplitude a_+ is given at the onset (recall the configurations in Fig. 1).

The hydrodynamic soliton tunneling problem then consists in finding (i) the transmitted soliton amplitude a_- and (ii) the stretching (contraction) coefficient k_+/k_- for the soliton train that determines the soliton phase shift due to tunneling. We will show that k_+/k_- is independent of the particular choice of k_+ (or, separately, k_-).

Concluding this section, we note that the long wave limit of the Whitham equations demonstrates that while the soliton amplitude is coupled to the evolving mean flow, the mean flow itself evolves *independently* of additional localized nonlinear waves.

III. HYDRODYNAMIC SOLITON TUNNELING

We shall consider the basic tunneling configurations depicted in Fig. 1, which are defined by constancy of the hydrodynamic Riemann invariant $\bar{r}$ in the step initial data (6). Without loss of generality, one can choose $(\bar{\rho}_-, \bar{u}_-) = (1,0)$, the remaining configurations can be deduced from scaling, Galilean shifts, and reflection symmetries associated with Eq. (2).

We note that, given step initial conditions, the hydrodynamic system (4) is valid only if the resulting wave is a RW. This implies that the reduced single-phase modulation system (4), (11), and (13) describes only soliton-RW interactions [cases (a) and (c) in Fig. 1]. Indeed, soliton DSW interaction is more complicated and generally requires consideration of two-phase NLS modulation equations [37]. Remarkably, however, we will show that the soliton-DSW tunneling conditions for cases (b) and (d) can be found from the soliton-RW tunneling conditions via *hydrodynamic reciprocity*.

Let us assume that $\bar{r}(x,0)$ has no jump across $x = 0$ and the jump in $\bar{s}(x,0)$ resolves into a RW. The modulation equations (4), (11), and (13) with step initial conditions for $\bar{s}$, r_3 and kp found from (6) and (14) imply the simple wave solution in which $\bar{r} = r_1$, r_3, and kp are constant for all (x,t) but $\bar{s} = r_4$ is varying in a self-similar fashion, $\bar{s} = \bar{s}(x/t)$. This 4-wave modulation solution describes the hydrodynamic tunneling configurations (a) and (c) in Fig. 1. An example 4-wave evolution is shown in Fig. 2.

The tunneling problem now essentially reduces to finding the constant values of r_3 and kp given the constant value of $\bar{r} = \bar{u}_+/2 - \sqrt{\bar{\rho}_+} = \bar{u}_-/2 - \sqrt{\bar{\rho}_-} = -1$ and the initial jump for $\bar{s}$ found from (6) so that the Riemann invariants resemble those in Fig. 2. The solution for $\bar{s}(x/t)$ will then define the soliton trajectory through a hydrodynamic RW barrier.
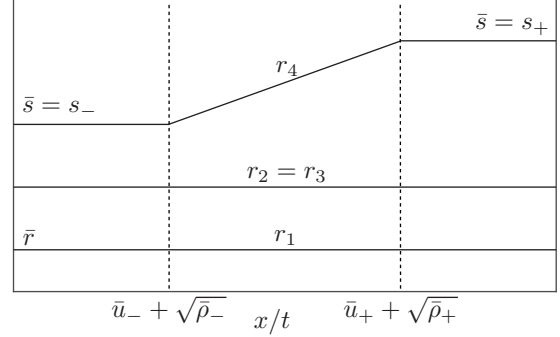
FIG. 2. Hydrodynamic soliton tunneling configuration of the Riemann invariants for soliton-RW interactions.

The requirement of constancy of r_3 defined by Eq. (12) when evaluated with (6) and (14) yields a simple algebraic expression for the transmitted soliton amplitude through a RW:

$$a_- = a_+ - 2(\sqrt{\bar{\rho}_+} \pm \sqrt{\bar{\rho}_+ - a_+})(\sqrt{\bar{\rho}_+} - 1). \qquad (15)$$

Importantly, tunneling through the hydrodynamic barrier requires $0 < a_- \leqslant 1$. The $\pm$ in Eq. (15) corresponds to the two branches of r_3 with "$-$" corresponding to the collision case depicted in Fig. 1(a) and "$+$" the overtaking case depicted in Fig. 1(c). The transmitted, or tunneled, soliton amplitude-speed relation is then

$$c_- = \pm\sqrt{1 - a_-}$$
$$= \frac{1}{2}(\bar{r} + r_3 + \bar{s}_-), \qquad (16)$$

with a_- given by Eq. (15). The expression for the soliton velocity c_- in terms of Riemann invariants is a convenient representation that inherently incorporates the appropriate sign $\pm$. We shall also explore implications of constancy of kp.

The formulas (15) and (16), in spite of their simplicity, exhibit a number of remarkable implications. These include soliton tunneling, soliton trapping, the spontaneous emergence of a cavitation point, and soliton direction reversal. Furthermore, the obtained conditions incorporate the fundamental notion of hydrodynamic reciprocity established for unidirectional systems of the Korteweg-de Vries (KdV) type in Ref. [31]. This states that the tunneling conditions *are the same for both the RW and DSW*. This concept enables the application of Eqs. (15) and (16) to soliton-DSW interaction.

To extend the reciprocity result of Ref. [31] to the hydrodynamic optical tunneling studied here, we consider a general case where the left background state is $(\bar{\rho}_-, \bar{u}_-)$ [not necessarily (1,0)] and take either $\bar{r}(x,0)$ or $\bar{s}(x,0)$ constant. This generalization will require consideration of both branches of r_3 in Eq. (12) and in the tunneling condition (15). Hydrodynamic reciprocity ultimately results from the time and space reversibility of the NLS equation (1).

We first consider the soliton-DSW interaction case where $\bar{\rho}_- > \bar{\rho}_+$ so that the DSW is known as a 2-DSW [23]. The soliton is initially located to the right of the DSW so that the hydrodynamic transition across the DSW satisfies a 4-wave modulation curve in which $\bar{r} = r_1 = $ const (see Refs. [23,35]):

$$\bar{u}_- - \bar{u}_+ = 2(\sqrt{\bar{\rho}_-} - \sqrt{\bar{\rho}_+}). \qquad (17)$$
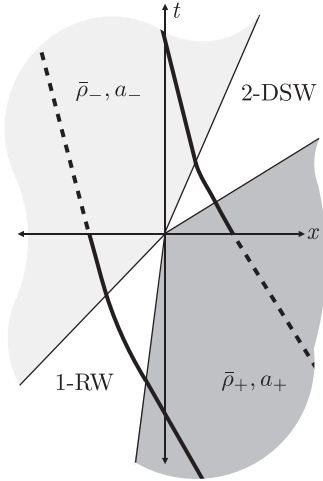
FIG. 3. Time reversibility of initial data $(\overline{\rho}_+, a_+)$ and $(\overline{\rho}_-, a_+)$ with $\overline{\rho}_+ < \overline{\rho}_-$. Forward temporal evolution results in soliton interaction with a 2-DSW (upper half plane), and backward evolution results in soliton interaction with a 1-RW. Soliton trajectories are depicted with solid and dashed curves.

The nonlinear superposition of a soliton and a DSW can be achieved by considering the modulation of two-phase (quasiperiodic) solutions of the NLS equation (1) [37]. Therefore, a description of the full soliton-DSW modulation would require the integration of the two-phase Whitham equations. However, we can determine all the results of soliton-DSW interaction by invoking continuity of the modulation solution for negative time.

If we now consider $t \to -t$ for the Whitham modulation equations (7), then the characteristic velocities $-V_i$ are reordered. The same initial data $\overline{\rho}_- > \overline{\rho}_+$ and the locus (17) corresponds to the generation of a 1-RW. If a soliton of amplitude a_- is initialized to the left of the RW, then soliton-RW interaction is determined by the constancy of r_3 so that the tunneled soliton amplitude satisfies

$$a_+ = a_- - 2(\sqrt{\overline{\rho}_-} \pm \sqrt{\overline{\rho}_- - a_-})(\sqrt{\overline{\rho}_-} - \sqrt{\overline{\rho}_+}), \quad (18)$$

where the $\pm$ corresponds to the same branch of r_3 that is taken. The relation (18) corresponds to a 1-wave modulation of the time-reversed Whitham equations. This is a global relationship that must also hold for the corresponding 4-wave soliton-DSW modulation of the nonreversed Whitham equations due to continuity of the modulation solution away from the origin. This analysis is pictured in Fig. 3, where, for negative time, a soliton-RW interaction is pictured and a soliton-DSW interaction is shown for positive time.

Equation (18) can be inverted to obtain a_- in terms of a_+ and $\overline{\rho}_\pm$. If we set $\overline{\rho}_- = 1$ and $\overline{u}_- = 0$, then Eq. (18) and Eq. (15) are equivalent. The tunneling condition (15) is the same for both soliton-RW and soliton-DSW interaction.

Another way to understand hydrodynamic reciprocity is schematically pictured in Fig. 4. Rather than reversing time, this figure depicts spatial reversal. A soliton of amplitude a_+ initially placed to the right of a jump with $\overline{\rho}_- < \overline{\rho}_+$ results in soliton interaction with a 2-RW and a_- satisfying Eq. (18). Now, consider a spatially reversed jump with $\tilde{\rho}_\pm = \overline{\rho}_\mp$ so
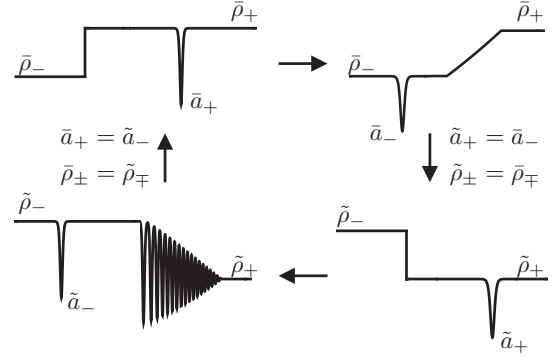
FIG. 4. Sketch of configurations demonstrating hydrodynamic reciprocity. Horizontal arrows refer to temporal evolution, and vertical arrows connote the transformation to the reciprocal initial condition.

that $\tilde{\rho}_- > \tilde{\rho}_+$. With a soliton of amplitude $\tilde{a}_+ = a_-$ initially placed on the right, the soliton interaction with a 2-DSW results in the tunneled amplitude $\tilde{a}_- = a_+$. This is the bidirectional generalization of the unidirectional hydrodynamic reciprocity condition noted in Ref. [31].

In what follows, we compare the modulation theory predictions for hydrodynamic optical soliton tunneling with numerical simulations of Eq. (1) for initial data comprised of a smoothed step Eq. (4) and a soliton. We use a standard sixth order finite difference spatial discretization with Dirichlet boundary conditions. Time evolution is achieved with the standard fourth order Runge-Kutta method. The numerical evolution was validated by the numerical evolution of the exact solitary wave solution on a uniform background (3).

Comparisons between the transmitted soliton amplitude predicted by Eq. (15) and numerical simulations are given in Fig. 5, showing excellent agreement. When the tunneling relation (15) is not satisfied for $a_\pm > 0$, the soliton will become trapped within the spatially extended hydrodynamic state. Trapping then results in the soliton acting as a nonlinear modulation of the hydrodynamic structure. Examples of a soliton trapped in a hydrodynamic barrier are shown in Fig. 6, where the soliton was unable to pass through the RW or DSW for long simulation times. Soliton-DSW trapping can be viewed as the formation of a "defect" in the locally periodic DSW structure, analogous to the soliton defects of KdV cnoidal waves considered in Ref. [40]. In contrast to classical optical soliton tunneling in which the localized pulse can be reflected by a barrier with sufficient energy, this is not possible in the context of hydrodynamic optical tunneling.

The simplest tunneling configuration is that of a solitary wave though a RW because the evolution of the macroscopic structure of the RW can be determined by standard methods applied to the modulation Eqs. (4) and (11). The RW evolution, in terms of the Riemann invariants, is

$$\overline{s}_{\mathrm{RW}}(x,t) = \begin{cases} \overline{s}_- & x < V_- t \\ \frac{1}{3}\left(2\frac{x}{t} - \overline{r}\right) & V_- t \leqslant x \leqslant V_+ t, \\ \overline{s}_+ & V_+ t < x \end{cases} \quad (19)$$

where $V(\overline{s},\overline{r}) = \frac{1}{2}(3\overline{s} + \overline{r})$ and $V_\pm = V(\overline{s}_\pm, \overline{r})$ are the edge speeds of the centered RW [34]. We note that small amplitude linear oscillations may be present at an edge of the RW in
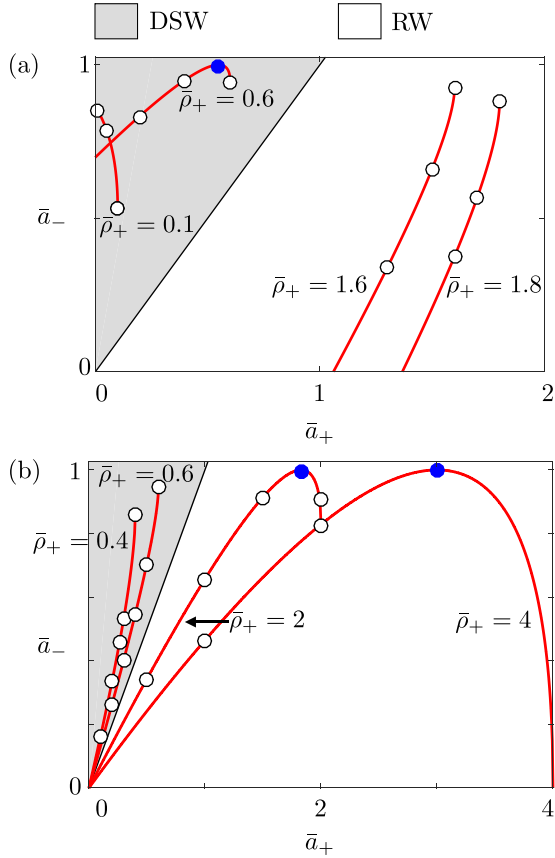
FIG. 5. Comparison between the tunneling relation (15) (solid curves) and direct numerical simulations of the NLS equation (dots) with smoothed, step initial data defined by $\bar{\rho}_+ > 0$ and a soliton of amplitude a_+. (a) The overtaking cases in Figs. 1(c) and 1(d). (b) The collision cases in Figs. 1(a) and 1(b). Filled dots correspond to the emergence of a black soliton. The grey regions correspond to soliton-DSW tunneling and white regions correspond to soliton-RW tunneling.

the full NLS dynamics due to dispersive regularization, but these oscillations decay and have negligible influence on the asymptotic RW behavior. The trajectory of the soliton center x_s is a characteristic (2- or 3-characteristic) of the Whitham

FIG. 6. Numerical simulation of hydrodynamically trapped solitons. (a) Soliton of amplitude $a_- = 0.25$ sent into a 2-DSW with $\bar{\rho}_+ = 0.5$. (b) Soliton of amplitude $a_+ = 1$ overtaken by RW with $\rho_+ = 4$.

modulation equations (7) that satisfies the initial value problem

$$\frac{dx_s}{dt} = c(\bar{r}, \bar{s}, r_3), \quad x_s(0) = x_+. \quad (20)$$

Here x_+ is the location of the solitary wave at $t = 0$ and the location of the step (6) is taken to be $x = 0$; c is the soliton amplitude-speed relation (16) written in terms of Riemann invariants. A direct integration of (20) results in the location of the solitary wave tunneling through a rarefaction wave

$$x_s(t) = \begin{cases} x_+ + c_+ t & x \leqslant t_1 \\ \dfrac{(\bar{r} + r_3)t + 3(\bar{s}_+ - r_3)t_1^{2/3}t^{1/3}}{2} & t_1 < x < t_2, \\ x_- + c_- t & t \geqslant t_2 \end{cases} \quad (21)$$

where

$$t_1 = x_+/(\bar{s}_+ - r_3),$$

$$t_2 = (\bar{s}_+ - r_3)^{3/2}(\bar{s}_- - r_3)^{-3/2}t_1,$$

$$x_- = (\bar{s}_+ - r_3)^{1/2}(\bar{s}_- - r_3)^{-1/2}x_+,$$

$$c_\pm = \tfrac{1}{2}(\bar{r} + 2r_3 + \bar{s}_\pm).$$

The effective phase shift of the soliton center through a RW is given by the difference in the x-intercepts of the linear soliton trajectories post- and pre-hydrodynamic interaction:

$$x_+ - x_- = \left(1 - \sqrt{\frac{\bar{s}_+ - r_3}{\bar{s}_- - r_3}}\right)x_+. \quad (22)$$

An alternative, instructive way to determine the interaction phase shift is to analyze the additional modulation equation (13) that describes the evolution of the wave number $0 < k \ll 1$ in a train of well-separated, noninteracting solitons with the amplitude field $a(x,t)$. Given the mean flow $\bar{s}_{\mathrm{RW}}(x,t)$ in (19), the amplitude field $a(x,t)$ is determined by the constancy of $\bar{r}$ and r_3 in Eq. (12). The soliton phase shift now follows from the requirement of constancy of the Riemann invariant pk of Eq. (13) across the initial step (6) and (14). Indeed, equating the values of pk at both sides of the initial step we find the ratio $k_+/k_- = x_-/x_+$, which determines the stretching (contraction) of the soliton wave train at leading order [31],

$$\frac{k_+}{k_-} = \frac{x_-}{x_+} = \exp\int_{\bar{s}_-}^{\bar{s}_+} \frac{\dfrac{dc}{d\bar{s}}}{\tfrac{1}{2}(\bar{r} + 3\bar{s}) - c}\, d\bar{s},$$

$$= \sqrt{\frac{\bar{s}_+ - r_3}{\bar{s}_- - r_3}}, \quad (23)$$

where the first term in the denominator is the characteristic speed associated with $\bar{s}$. This simpler approach yields the same result as that obtained in Eq. (22) from Eq. (21).

We can now invoke the notion of hydrodynamic reciprocity—the surprising fact that the interaction of the soliton with a RW is the same as that with a DSW at the macroscopic level. In addition to the tunneling relation (15), the phase shift (22) also applies to soliton-DSW interaction. The macroscopic properties of the DSW itself—leading harmonic edge speed and trailing soliton edge speed—are determined by an analysis of the single phase Whitham equations in place of
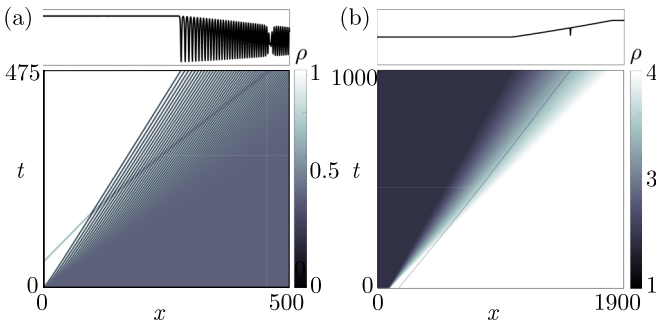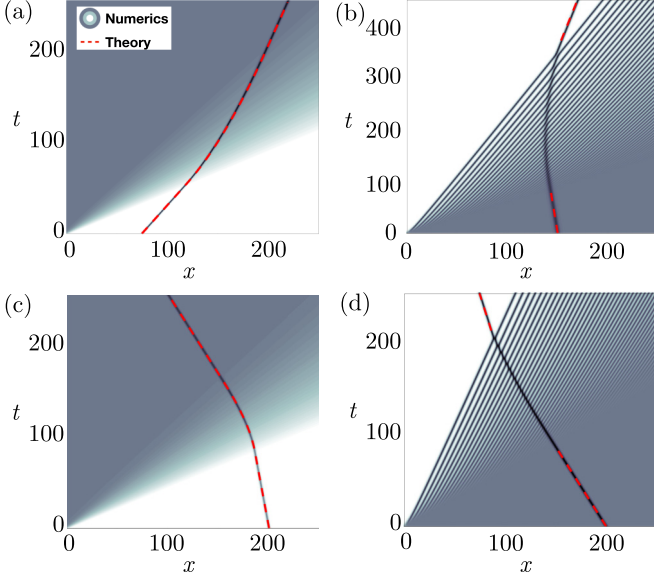
FIG. 7. Tracking a soliton through a RW and DSW via Eqs. (21) and (25). (a) $\overline{\rho}_+ = 2$, $a_+ = 1$ and the sign of r_3 in Eq. (12) is "$-$." (b) $\overline{\rho}_+ = 0.5$, $a_+ = 0.5$, the r_3 sign is "$-$." (c) $\overline{\rho}_+ = 2$, $a_+ = 2$, the sign of r_3 is "$+$." (d) $\overline{\rho}_+ = 0.5$, $a_+ = 0.4$, the sign of r_3 is "$+$." Predictions from Eqs. (21) and (25) are the red dashed curves, the contours are from direct numerical simulation of Eq. (1).

the direct integration that was possible in the RW case. The distinguished edge speeds of the DSW are given by [41,43]

$$V_{-,\text{DSW}} = 2\sqrt{\overline{\rho}_+} - 1,$$
$$V_{+,\text{DSW}} = \bar{u}_+ + \frac{\overline{\rho}_+ - 8\sqrt{\overline{\rho}_+} + 8}{2 - \sqrt{\overline{\rho}_+}}. \tag{24}$$

Incorporating the soliton phase shift Eq. (23) results in the soliton trajectory before and after interaction

$$x_{s,\text{DSW}} = \begin{cases} x_+ + \frac{1}{2}(\bar{r} + 2r_3 + \bar{s}_+)t, & x \leqslant t_1 \\ x_- + \frac{1}{2}(\bar{r} + 2r_3 + \bar{s}_-)t, & x \geqslant t_2 \end{cases}, \tag{25}$$

where now, t_1, t_2 are determined by equating the pre and post-interaction soliton trajectories with the appropriate DSW edge velocities from Eq. (24). Comparisons with numerical simulations of soliton-DSW interactions are shown in Figs. 7(b) and 7(d) with excellent agreement. The trajectory prediction Eq. (25) also correctly captures the phenomenon of soliton direction reversal shown in Fig. 7(d).

The transition to a different mean flow across the hydrodynamic barrier not only results in a controllable soliton trajectory but also the generation of transmitted solitons of pre-specified amplitudes [cf. Eq. (15)]. For specific initial configurations of the tunneling problem, we predict and numerically observe the spontaneous development of a black soliton that exhibits cavitation or a null in the density at the soliton minimum which is demonstrated in Fig. 8. Black soliton solutions are characterized in the normalization considered here by an amplitude $a_- = 1$ with an associated π phase jump across the soliton minimum. In the reference frame chosen, the soliton velocity on the left flow is given by $c_- = 0$. The phenomenon of so-called self cavitation of dispersive shock waves was
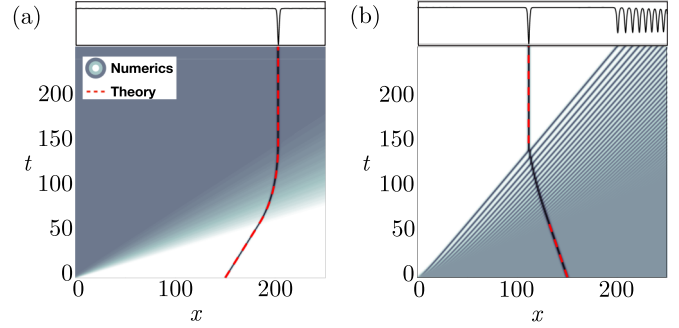
FIG. 8. Examples of the emergence of a black soliton after tunneling in the characteristic plane. The initial configurations are (a) RW collision case with $\overline{\rho}_+ = 2$, (b) DSW overtaking case with $\overline{\rho}_+ = 0.6$. Initial soliton amplitudes are chosen so that $a_- = 1$ in (15). Numerically computed soliton trajectories (contours) are compared against theoretical predictions of Eqs. (21) and (25). The snapshots of the intensity ρ at $t = 225$ are shown above the contour plots.

theoretically predicted in [35] and both a zero density point and the associated π phase jump was observed experimentally for the dam break problem of spin waves in a defocusing magnetic material [42]. Zero density points were also observed in an optical "photon fluid" [22]. The interaction of a dark soliton with a mean flow then gives a fundamentally new mechanism for generating a cavitation point in the flow.

IV. CONCLUSION

In this work, we have introduced a notion of hydrodynamic optical soliton tunneling where a localized, depression wave or dark soliton is incident on a spatiotemporal hydrodynamic barrier. Under the assumptions of nonlinear wave, Whitham modulation theory, the evolution of the inhomogeneous mean flow decouples from the soliton so that, at the leading order macroscopic level, the flow is wholly unaltered by the presence of the local pulse. The solution is found to be a self-similar simple wave of a system of quasilinear partial differential equations whose characteristics determine both the mean flow and the soliton trajectory. The self-similar simple wave obtained evolves from an initial step in the flow to either a single DSW or a RW but the approach generalizes to any initial state that limits to different constants as $x \rightarrow \pm \infty$, which define soliton tunneling conditions.

The main result of this work is encompassed in the tunneling and phase relations given by Eqs. (15) and (23). They determine the transmitted soliton amplitude, speed, and position in terms of only the incident soliton amplitude, its position, and the hydrodynamic flow in the far field. The known soliton trajectory and amplitude following interaction provide a mechanism for soliton control via interaction with a spatially extended mean flow.

The notion of hydrodynamic reciprocity identified earlier in Ref. [31] for scalar, KdV-type systems and generalized here to the NLS case allows one to investigate a complex soliton-DSW interaction by studying the simpler case of soliton-RW interaction. Reciprocity implies that, although the tunneling of a soliton through a DSW involves a complex interaction with rapid nonlinear oscillations, they are unimportant for

determining the resulting amplitude, velocity and shift of the solitary wave post-interaction. The methodology presented here to track the trajectory of the soliton only requires knowledge of the far field boundary conditions and hence this approach can be extended to other initial configurations. We also note that the developed theory is not restricted to integrable NLS dynamics and can be generalized to other cases of hydrodynamic optical soliton tunneling described by nonintegrable versions of the defocusing NLS equation, e.g., with saturable nonlinearity, using the methods of Refs. [23,32,44].

ACKNOWLEDGMENTS

[1] L. Landau and E. Lifshitz, *Quantum Mechanics* (Pergamon Press, Oxford, 1965).

[2] A. C. Newell, J. Math. Phys. **19**, 1126 (1978).

[3] V. N. Serkin, V. A. Vysloukh, and J. R. Taylor, Electron. Lett. **29**, 12 (1993).

[4] D. Anderson, M. Lisak, B. Malomed, and M. Quiroga-Teixeiro, J. Opt. Soc. Am. B **11**, 2380 (1994).

[5] W.-P. Zhong and M. R. Belić, Phys. Rev. E **81**, 056604 (2010).

[6] J. Wang, L. Li, and S. Jia, J. Opt. Soc. Am. B **25**, 1254 (2008).

[7] R. Yang and X. Wu, Opt. Express **16**, 17759 (2008).

[8] G. Assanto, A. A. Minzoni, M. Peccianti, and N. F. Smyth, Phys. Rev. A **79**, 033837 (2009).

[9] M. Peccianti, A. Dyadyusha, M. Kaczmarek, and G. Assanto, Phys. Rev. Lett. **101**, 153902 (2008).

[10] M. I. Rodas-Verde, H. Michinel, and V. M. Pérez-García, Phys. Rev. Lett. **95**, 153903 (2005).

[11] S. Loomba, H. Kaur, R. Gupta, C. N. Kumar, and T. S. Raju, Phys. Rev. E **89**, 052915 (2014).

[12] Y. Linzon, R. Morandotti, M. Volatier, V. Aimez, R. Ares, and S. Bar-Ad, Phys. Rev. Lett. **99**, 133901 (2007).

[13] A. Barak, O. Peleg, C. Stucchio, A. Soffer, and M. Segev, Phys. Rev. Lett. **100**, 153901 (2008).

[14] T. Marest, F. Braud, M. Conforti, S. Wabnitz, A. Mussot, and A. Kudlinski, Opt. Lett. **42**, 2350 (2017).

[15] T. L. Belyaeva and V. N. Serkin, Euro. Phys. J. D **66**, 153 (2012).

[16] V. N. Serkin, A. Hasegawa, and T. L. Belyaeva, J. Mod. Opt. **60**, 116 (2013).

[17] V. N. Serkin, A. Hasegawa, and T. L. Belyaeva, J. Mod. Opt. **60**, 444 (2013).

[18] V. Zakharov and L. Ostrovsky, Physica D **238**, 540 (2009).

[19] I. Carusotto and C. Ciuti, Rev. Mod. Phys. **85**, 299 (2013).

[20] W. Wan, S. Jia, and J. W. Fleischer, Nat. Phys. **3**, 46 (2007).

[21] J. Garnier, G. Xu, S. Trillo, and A. Picozzi, Phys. Rev. Lett. **111**, 113902 (2013).

[22] G. Xu, M. Conforti, A. Kudlinski, A. Mussot, and S. Trillo, Phys. Rev. Lett. **118**, 254101 (2017).

[23] G. A. El and M. A. Hoefer, Physica D **333**, 11 (2016).

[24] C. Conti, A. Fratalocchi, M. Peccianti, G. Ruocco, and S. Trillo, Phys. Rev. Lett. **102**, 083902 (2009).

[25] B. Wetzel, D. Bongiovanni, M. Kues, Y. Hu, Z. Chen, S. Trillo, J. M. Dudley, S. Wabnitz, and R. Morandotti, Phys. Rev. Lett. **117**, 073902 (2016).

[26] G. Biondini, G. El, M. Hoefer, and P. Miller, Physica D **333**, 1 (2016).

[27] G. B. Whitham, *Linear and Nonlinear Waves* (Wiley, New York, 1974).

[28] N. J. Zabusky and M. D. Kruskal, Phys. Rev. Lett. **15**, 240 (1965).

[29] M. J. Ablowitz and Y. Kodama, Stud. Appl. Math. **66**, 159 (1982).

[30] R. W. Boyd, *Nonlinear Optics* (Academic Press, San Diego, 2013).

[31] M. D. Maiden, D. V. Anderson, N. A. Franco, G. A. El, and M. A. Hoefer, Phys. Rev. Lett. (to be published).

[32] M. A. Hoefer, J. Nonlinear Sci. **24**, 525 (2014).

[33] L. P. Pitaevskii and S. Stringari, *Bose-Einstein Condensation* (Clarendon, Oxford, 2003).

[34] R. J. LeVeque, *Finite Volume Methods for Hyperbolic Problems* (Cambridge University Press, Cambridge, 2002).

[35] G. A. El, V. V. Geogjaev, A. V. Gurevich, and A. L. Krylov, Physica D **87**, 186 (1995).

[36] M. V. Pavlov, Theor. Math. Phys. **71**, 584 (1987).

[37] M. G. Forest and J. Lee, *Oscillation Theory, Computation, and Methods of Compensated Compactness*, edited by C. Dafermos *et al.* (Springer, New York, 1986), Vol. 2, pp. 35–69.

[38] A. M. Kamchatnov, *Nonlinear Periodic Waves and Their Modulations: An Introductory Course* (World Scientific, Singapore, 2000).

[39] Y. S. Kivshar and B. A. Malomed, Rev. Mod. Phys. **61**, 763 (1989).

[40] E. Kuznetsov and A. Mikhailov, Sov. J. Exp. Theor. Phys. **40**, 855 (1975).

[41] A. V. Gurevich and A. L. Krylov, Sov. Phys. JETP **65**, 944 (1987).

[42] P. A. P. Janantha, P. Sprenger, M. A. Hoefer, and M. Wu, Phys. Rev. Lett. **119**, 024101 (2017).

[43] M. A. Hoefer, M. J. Ablowitz, I. Coddington, E. A. Cornell, P. Engels, and V. Schweikhard, Phys. Rev. A **74**, 023623 (2006).

[44] G. A. El, Chaos **15**, 037103 (2005).